CIGRE SESSION 48

B4 - 328

Paris 2020

Improving synthetic inertia provision by power electronic interfaced power sources to support future system stability

W. GAWLIK, C. ALACS, J. MARCHGRABER, Y. GUO, A. ANTA, J. KATHAN, B. WEISS, K. OBERHAUSER, M. LENZ, M. FROSCHAUER, A. STIMMER, M. LEONHARDT
TU Wien, AIT Austrian Institute of Technology, VERBUND Solutions GmbH, VERBUND Hydro Power, Austrian Power Grid AG
Austria

SUMMARY

Increasing penetration of power electronics converter interfaced generation and loads raises several challenges for the operation, control and protection of power systems. This paper investigates the impact of high penetration of power electronic interfaced power sources (PEIPS) on frequency control, and aspects of provision of synthetic inertia (SI) by PEIPS. Contrary to directly connected conventional synchronous machines, which provide inertia to the system inherently, thus effectively counteracting large gradients in the system frequency (rate of change of frequency, RoCoF), PEIPS need to be operated under specially designed control schemes, in order to provide synthetic inertia by varying their power output proportionally to the RoCoF. Implementing such control schemes for current-controlled PEIPS requires both accurate and fast frequency measurement and can rather approximate than reproduce physical inertia added to the system by directly connected synchronous machines. While the transient behavior of conventional synchronous machines is defined by their well-known electromechanical properties, the dynamic behavior of PEIPS is mostly dictated and limited by their control strategy and pertinent measurements. Under this setup, it is worth contemplating strategies that go beyond mimicking the dynamic capabilities of synchronous machines. A synchronous machine provides inertia to the system inherently due to its rotating mass. However, current-controlled PEIPS, implement synthetic inertia by measuring frequency, calculating the frequency gradient and providing power accordingly. The delays due to frequency measurement, RoCoF computation and current control reflect an inherent difference and disadvantage of synthetic inertia compared to real inertia and must be properly studied to avoid deterioration of system stability under a large penetration of PEIPS. While the behavior of synchronous machines is determined by their physical properties, the behavior of PEIPS may be altered by modifying their control regime in order to improve their transient behavior under higher RoCoF values. Furthermore, it is possible to implement non-linear strategies that do not depend only on the frequency gradient, but also on the frequency deviation. One option to achieve this is to implement different activation areas for different signs of both

gawlik@ea.tuwien.ac.at

frequency deviation and RoCoF. Such a zone-selective implementation of synthetic inertia, realized by an activation function, could avoid that synthetic inertia counteracts the effect of other control reserves during recovery from frequency deviations, i.e. after the frequency nadir has occurred. This paper investigates such options and their impact on the frequency stability of the power system when synthetic inertia is provided by PEIPS.

KEYWORDS

Synthetic inertia (SI), zone-selective activation, power electronic interfaced power sources (PEIPS)

Introduction

Historically, the electrical power supply is primarily based on centralized power plants, which are feeding into the grid via synchronous machines. These synchronous machines possess a rotating mass that helps to limit the rate of change of frequency (RoCoF) in case of power imbalances in the system. However, recent trends show a decrease of the number of conventional power plants and an increasing penetration of power electronic interfaced power sources (PEIPS) [1]. Unlike synchronous machines, PEIPS do not provide any form of inertia, unless they are operated under specially designed control schemes. Therefore, this trend leads to a decrease of system inertia and poses new challenges regarding frequency stability [2]. Measures of system inertia are the system inertia constant (H) and the network time constant (T_A), which corresponds to twice the value of H. Figure 1 shows the predicted values of the network time constant over the period of one year for 2030 and 2040 for different scenarios according to [3].

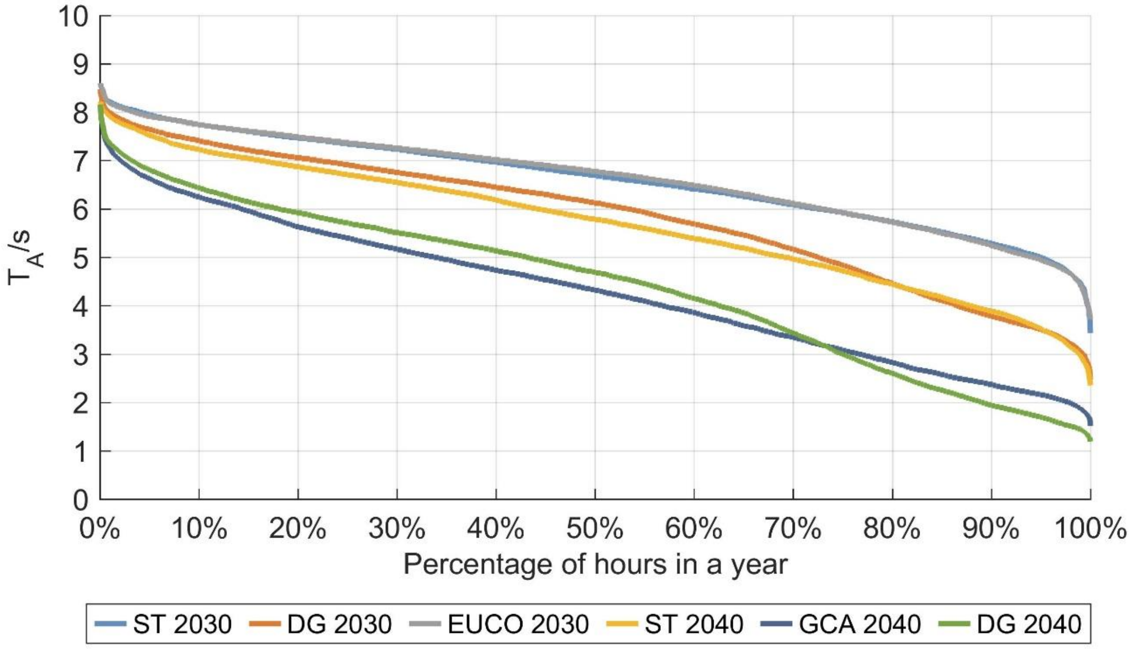

Figure 1: Predicted values of the network time constant (T_A) over the period of one year for 2030 and 2040 for different scenarios[1] (based on [3])

The decreasing network time constant causes growing issues regarding frequency stability and control, and raises the question of whether the current balancing reserves will be sufficient in the future to stabilize the frequency in case of a reference incident, similar to the "design hypothesis" [4]. Figure 2 presents frequency curves for a reference incident and different values of the assumed network time constant (T_A). Figure 2 shows that for values of $T_A < 10\,s$ the frequency drops below 49.2 Hz, which is the current dynamic frequency limit in the synchronous area of Continental Europe (CE), and for values of $T_A < 6\,s$, the frequency drops below 49 Hz, which is the current limit for load shedding in CE. Since such T_A values are shown as likely for the future, the use of faster frequency reserves will be required. Within the project "ABS4TSO" [5], the possible implementation and

[1] Scenario ST: sustainable transition; DG: distribution generation; EUCO: policy provided by European Commission; GCA: global climate action

requirements for such reserves in the CE are investigated. This paper focuses on provision of synthetic inertia (SI) by PEIPS and possible improvements of synthetic inertia compared to real inertia.

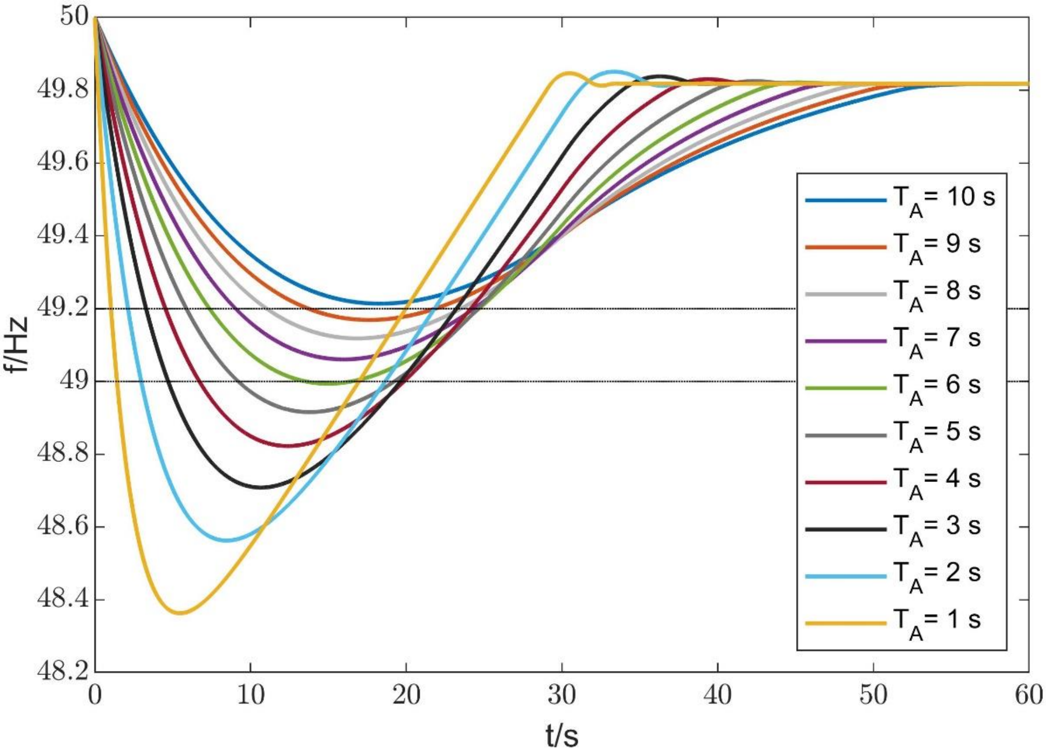

Figure 2: Frequency curves for a reference incident according to the "design hypothesis" [4] (System size: 150 GW, self-regulating effect of the loads: 1%/Hz, power imbalance: 3 GW) dependent on the network time constant (T_A)

Methodology

Initially, the frequency and time characteristic curves for provision of synthetic inertia as well as the range of the related parameters were defined. Next, a model of the synthetic inertia provision was built in MATLAB/SIMULINK and incorporated in a single-area model for CE. With this model, an initial system analysis was conducted to assess the impact of synthetic inertia on frequency excursions, caused by the reference incident. Then, a sensitivity analysis was carried out in order to determine the impact of each parameter of the synthetic inertia model on the power and frequency characteristics. In addition, the sensitivity analysis should also assess sensible intervals for each parameter and allow for a first evaluation on the effectiveness of synthetic inertia as a fast frequency supporting service. Following, the differences between real and synthetic inertia were highlighted and examinations were performed on whether synthetic inertia can be improved by only adopting the advantageous characteristics of real inertia. For this, a zone-selective activation and deactivation of synthetic inertia is introduced in this paper. Finally, investigations on the impact of this zone-selective control are conducted and a possible parametrization of such an activation characteristic is discussed.

Characteristic curves and parameters of synthetic inertia

Figure 3(a) and Figure 3(b) show the synthetic inertia characteristic curves for the implemented model. Table 1 presents the parameter values used for the initial system dynamics simulations as well as the intervals to be investigated in further research. In this model, the synthetic inertia power is activated whenever both the frequency and frequency gradient are outside their respective deadbands Δf_{db} and $(\Delta f/\Delta t)_{db}$. P_{SImax} represents the power activated at the frequency gradient of $(\Delta f/\Delta t)_{max}$. The corresponding actual power output (P_{SI}), based on a steady state setpoint of the power ($P_{SI,ss}$) for an actual frequency gradient ($\Delta f/\Delta t$) at them time T_{curr}, is approximated according to the PT1 characteristic shown in Figure 3(b).

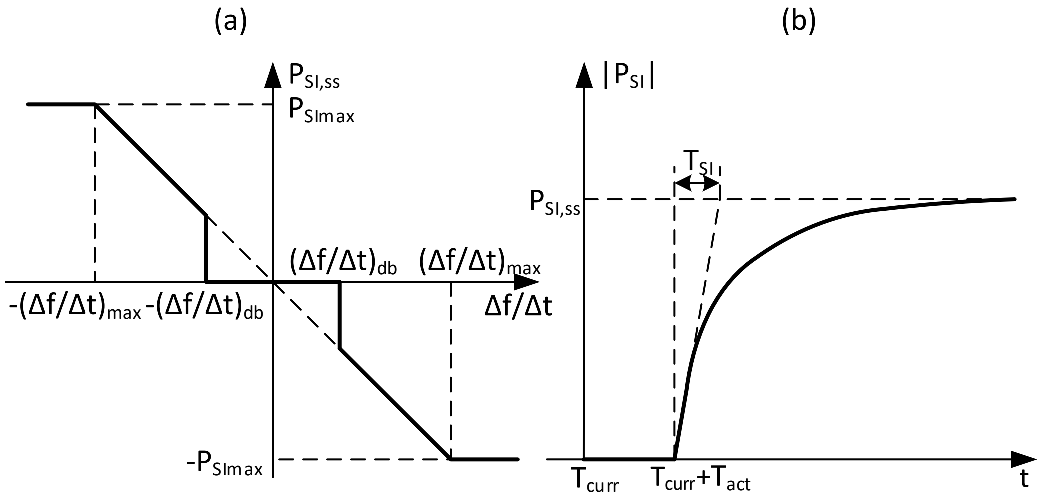

Figure 3: (a) Synthetic inertia characteristic curve dependent on the frequency gradient, (b) Synthetic inertia characteristic curve dependent on the time

Table 1: Parameter values for the synthetic inertia model

Parameter	Unit	Reference values	Interval
Δf_{db}	Hz	0.01	(0.01;0.20)
$(\Delta f/\Delta t)_{db}$	Hz/s	0.01	(0.01;2.00)
T_{act}	s	0.50	(0.00;1.00)
T_{SI}	s	2.00	(0.50;5.00)
$(\Delta f/\Delta t)_{max}$	Hz/s	0.20	(0.10;4.00)
P_{SImax}	MW	-	n.a.

The power values are determined for selected scenarios via simulations with the single-mass model, by identifying the required power to maintain a frequency above 49.2 Hz. The results of the initial system dynamics analysis, for a reference incident according to [4], but with a starting time constant of $T_A = 5\,s$, are presented in Figure 4. The trend for P_{FCR} (Frequency Containment Reserve, FCR) in Figure 4 is the same for both cases ("Only FCR" and "FCR and SI"); SI is only active during the second case ("FCR and SI").

Figure 4 shows that synthetic inertia can improve frequency stability and thus can help to keep the frequency above the 49.2 Hz frequency limit. Furthermore, it is clearly visible that synthetic inertia improves the inertial response of the system as it limits the frequency gradient and delays the frequency nadir. However, it also delays the frequency recovery after the nadir, since it limits the frequency gradient during the recovery period as well. Moreover, it can be observed that FCR and SI have the same direction, immediately after the reference incident, but that beginning around 20s after the reference incident, SI counteracts FCR, thus making FCR less effective.

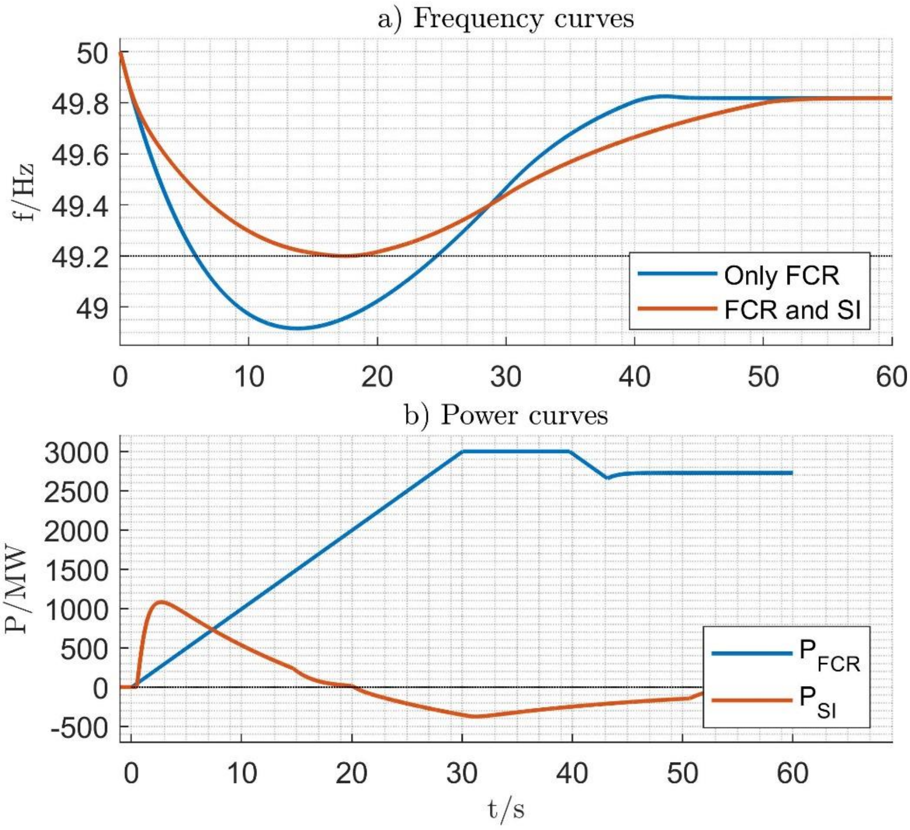

Figure 4: Frequency and power curves following a reference incident with and without synthetic inertia

Sensitivity analysis

In order to gain a deeper understanding of the operation of synthetic inertia and assess the impact of its parameters, a sensitivity analysis has been conducted. The following section presents an excerpt of this analysis, for the reference incident and a network time constant of $T_A = 5\ s$. The parameters used for the synthetic inertia correspond to the reference values from Table 1 with $P_{SImax} = 2550\ MW$. In each of the following figures, the results for the reference value of the respective parameter are presented first, followed by selected values within the specified range of values from Table 1.

Figure 5 shows the impact of the frequency deadband on the frequency and power curves. As depicted, the frequency deadband has almost no impact on the operation of synthetic inertia for values Δf_{db} ≤100 mHz and only a limited effect for Δf_{db} =200 mHz. On the other hand, the frequency gradient deadband $(\Delta f/\Delta t)_{db}$ has a major impact on the frequency and power curves. The corresponding curves are presented in Figure 6. Higher values for the parameter $(\Delta f/\Delta t)_{db}$ result in an earlier deactivation of synthetic inertia and thus a limited frequency support. For even higher values (see $(\Delta f/\Delta t)_{db}$ > 1 Hz/s in Figure 6), synthetic inertia is not even activated in this setting.

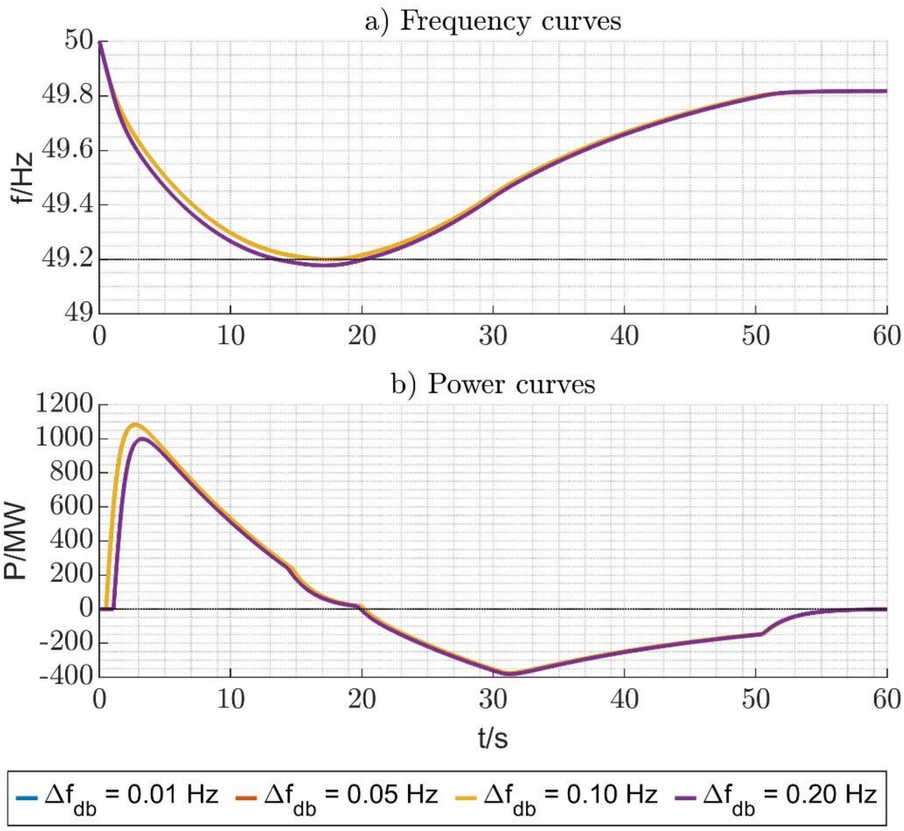

Figure 5: Frequency and power curves for the investigated reference incident and different values of Δf_{db}

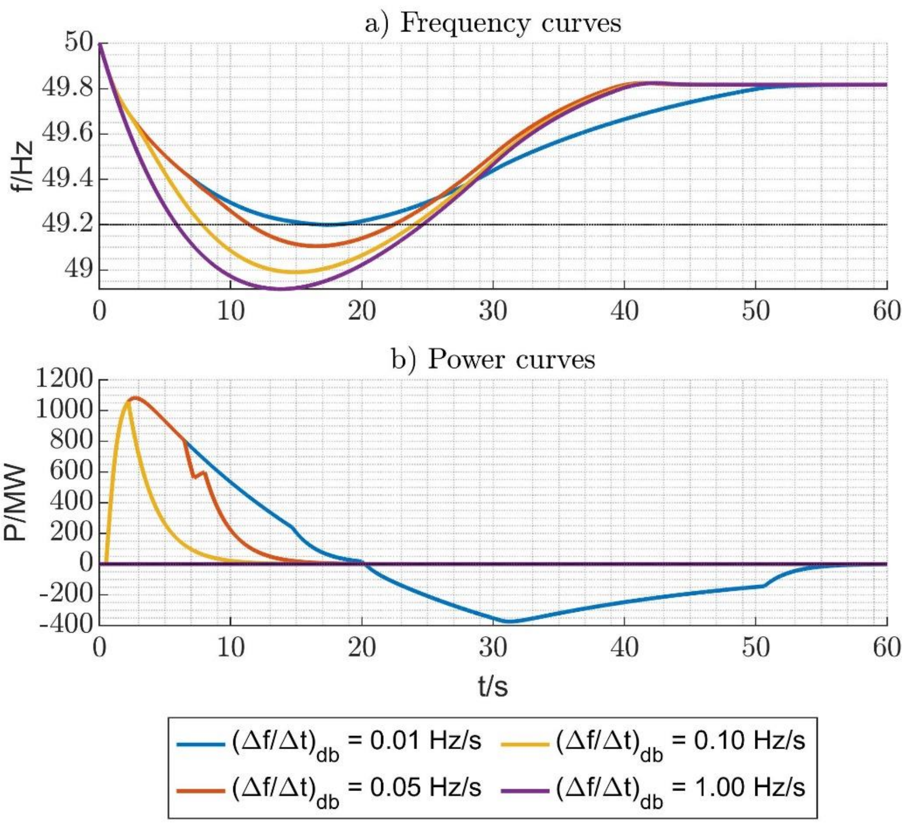

Figure 6: Frequency and power curves for the investigated reference incident and different values of $(\Delta f/\Delta t)_{db}$

Figure 6 highlights one of the challenges of parametrizing synthetic inertia. For the case with $(\Delta f/\Delta t)_{db}$=0.05 Hz/s, the change in RoCoF caused by deactivating synthetic inertia, is enough to move the RoCoF outside the frequency gradient deadband and reactivate synthetic inertia. Obviously, discontinuous characteristic curves for synthetic inertia should be avoided to avoid this effect.

Figure 7 shows the effect of the parameter T_{act}, which is composed of the frequency measurement time, the frequency gradient calculation time and the current control time, on the frequency and power curves. As shown in the figure, the results are relatively similar and the impact of T_{act} is negligible in case of the investigated reference incident. However, it must be noted that the reference incident presents a special case, in which the frequency decreases monotonously until it reaches the frequency nadir and increases monotonously afterwards. During normal operation of the power system, the frequency behaves differently, as it globally oscillates around certain mean values near 50 Hz and locally oscillates against the center of gravity in multi-mass systems. Because of the higher dynamics of the frequency and its gradient, the requirements found for T_{act} would also be much stricter when investigating normal operation.

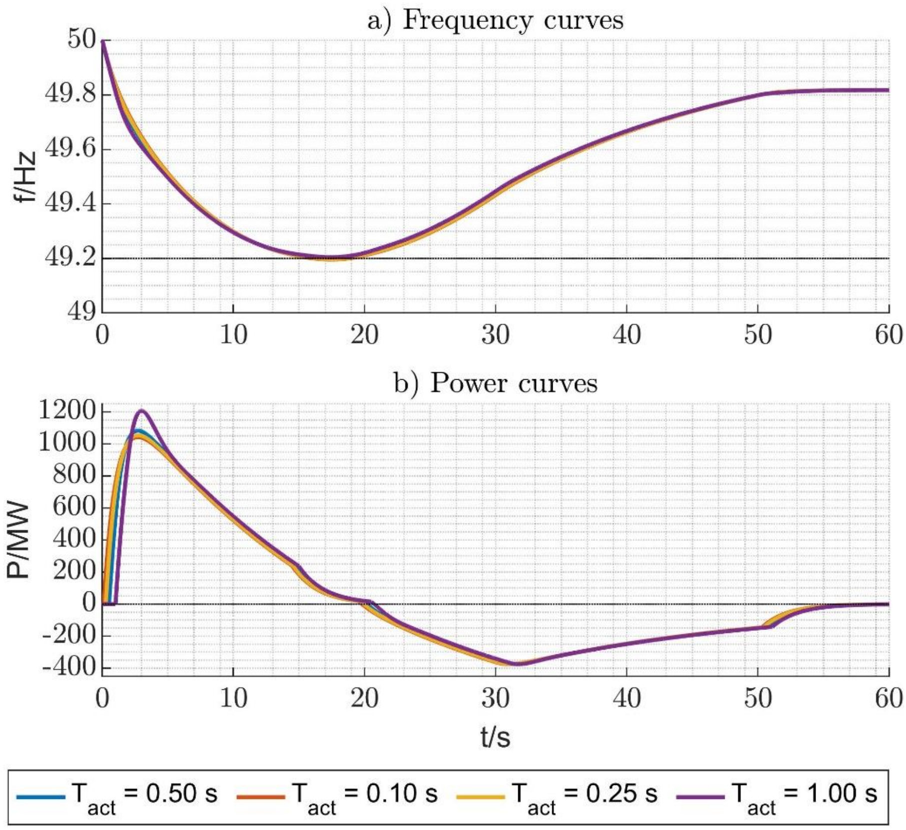

Figure 7: Frequency and power curves for the investigated reference incident and different values of T_{act}

The impact of the parameter T_{SI} is depicted in Figure 8. As shown, the parameter does not affect the frequency significantly but it has noticeable impact on the power curve. For greater values of T_{SI}, the power provided by synthetic inertia changes more slowly, so that the maximum SI power decreases and positive power is provided for a slightly longer period. This leads to a higher value of the frequency at an earlier frequency nadir.

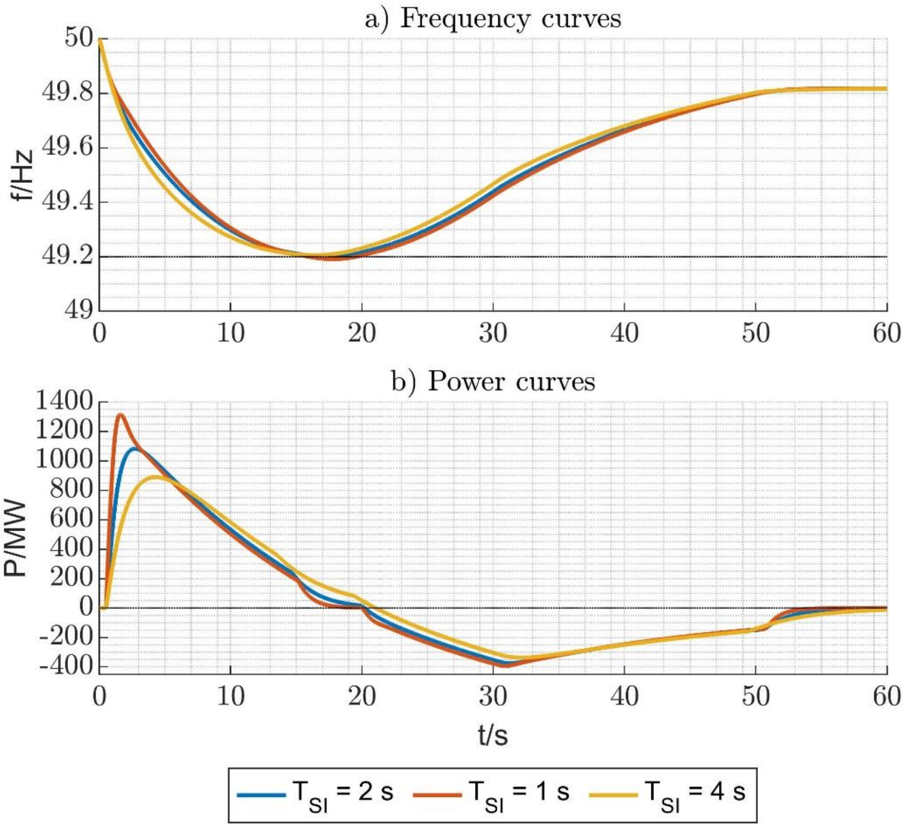

Figure 8: Frequency and power curves for the investigated reference incident and different values of T_{SI}

Finally, Figure 9 shows the effect of the parameter $(\Delta f/\Delta t)_{max}$. As displayed, the parameter has a major impact on both the frequency and power curves. In case of greater values of $(\Delta f/\Delta t)_{max}$, only a small portion P_{SI} of the synthetic inertia power P_{SImax} is provided and the frequency cannot be stabilized above 49.2 Hz. For smaller values, however, the change in RoCoF, in consequence of a change in power provided by the synthetic inertia, has a significant magnitude and can lead to chattering (especially around the frequency gradient deadband), as can be observed in Figure 9 for $(\Delta f/\Delta t)_{max}$ = 0.10 Hz/s around the frequency nadir and around 50 s.

The results of the sensitivity analysis have shown that the impact of the parameters Δf_{db}, T_{act} and T_{SI} is almost negligible and the intervals as well as the initial values provided in Table 1 present sensible assumptions. On the other hand, the two parameters $(\Delta f/\Delta t)_{db}$ and $(\Delta f/\Delta t)_{max}$ have a significant impact on the operation and effectiveness of synthetic inertia and need to be adjusted rather carefully. However, there is a notable difference between the two parameters. The parameter $(\Delta f/\Delta t)_{db}$ can be set to a specific value (e.g. 0.01 Hz/s) and synthetic inertia will behave the same way for small power imbalances as it would in case of a reference incident or a system split. In contrast to this, the impact of $(\Delta f/\Delta t)_{max}$ depends on the power imbalance at hand. For instance, a value of $(\Delta f/\Delta t)_{\max} = 0.2\ Hz/s$ might prove suitable for smaller power imbalances and the investigated reference incident, but could cause oscillations in case of a system split, while a greater value might prevent oscillations, but does not result in enough power in case of small power imbalances.

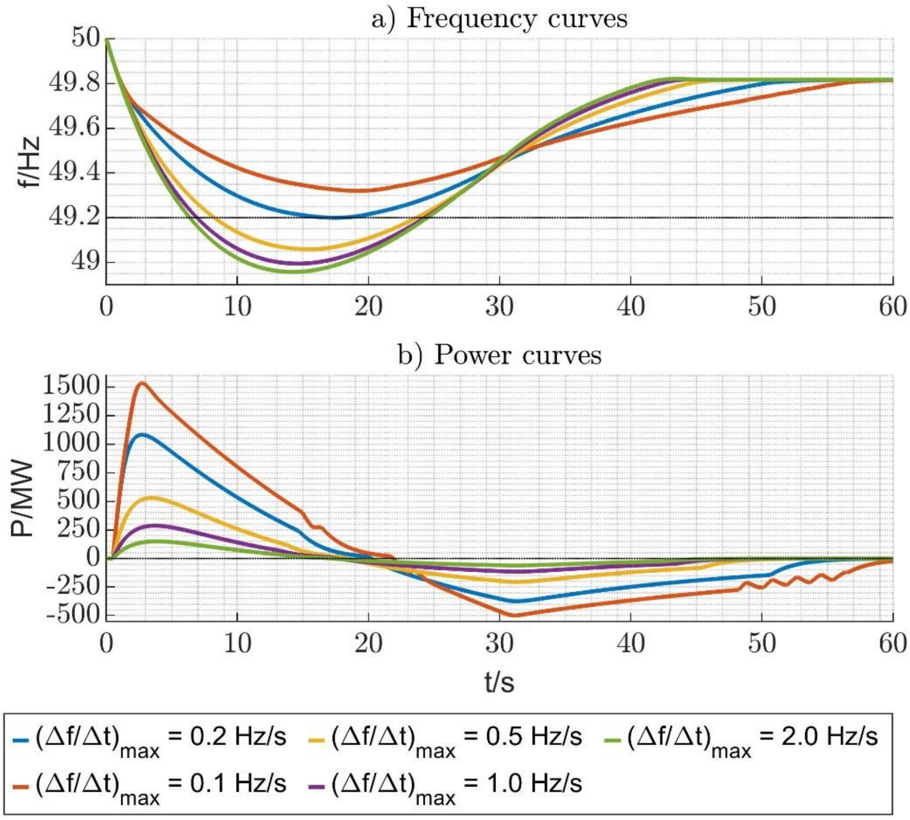

Figure 9: Frequency curves for the investigated reference incident and different values of $(\Delta f/\Delta t)_{max}$

Zone-selective activation and deactivation

Since many PEIPS do not provide synthetic inertia inherently but rather try to emulate real inertia provided by synchronous machines, their behavior may be altered by modifying their control scheme in order to improve its effectiveness. One option to achieve this is to implement a zone-selective control of synthetic inertia, dependent on both the frequency deviation (Δf) and the frequency gradient ($\Delta f/\Delta t$). Following, three options for the implementation of a zone-selective control are presented. The first option of such a zone-selective control is depicted in Figure 10.

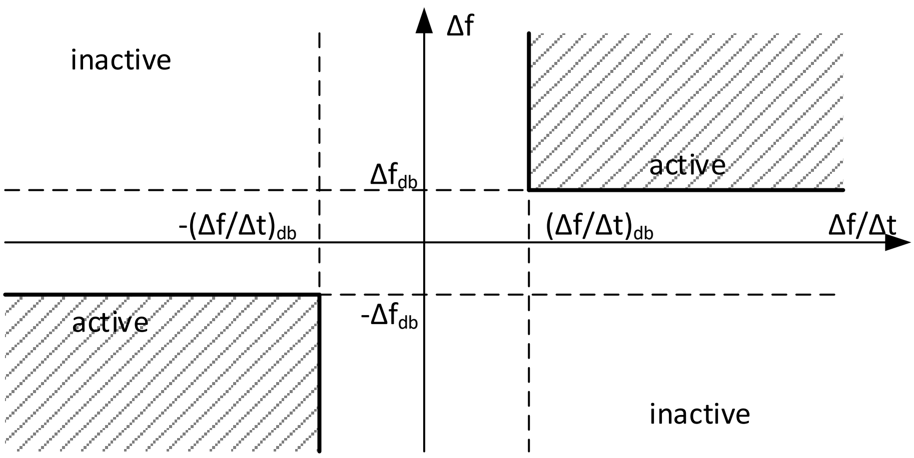

Figure 10: First option for the implementation of a zone-selective control (v1)

As can be seen, the synthetic inertia is only active if both the frequency deviation and gradient are outside their respective deadbands and have the same sign, resulting in a frequency moving away from 50 Hz. Whenever the frequency deviation and the frequency gradient have a different sign, synthetic inertia is inactive. In this way, synthetic inertia is not active during a recovery period, when the frequency is moving towards 50 Hz. Figure 11 shows the frequency and power curves with and without zone-selective control of synthetic inertia. It is clearly visible that with zone-selective control, no power is provided after the frequency nadir and the frequency recovery period is shorter. Due to this control scheme, the synthetic inertia stabilizes the frequency and supports its recovery. Furthermore, this behavior eliminates the possibility that two units, one providing a frequency reserve like FCR, the other providing synthetic inertia, could end up exchanging energy between each other without supporting the frequency restoration at all.

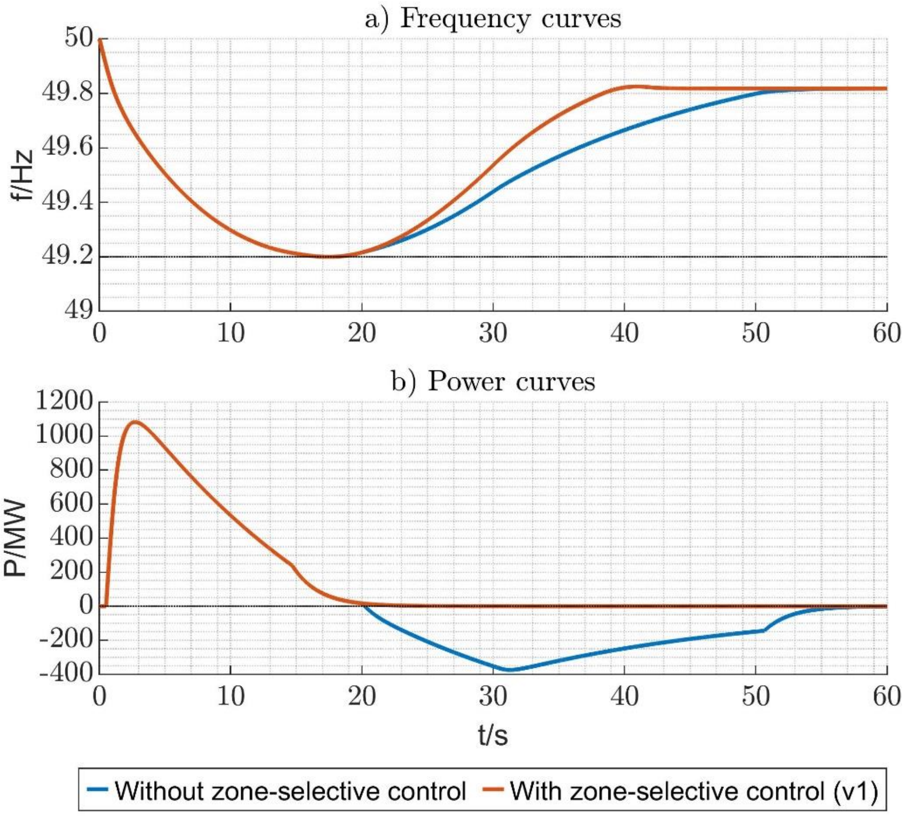

Figure 11: Frequency curves with and without zone-selective control (v1)

However, the control scheme presented in Figure 10 has a disadvantage in case of under- or overshooting frequency events, since it does not provide inertia during the recovery period. Figure 12 shows an improved version of the zone-selective control that tries to compensate this effect to some extent, by considering the progression of frequency during the time of T_{act}. At every given moment T_{curr}, the method calculates the frequency deviation, based on the current frequency gradient, for the moment $T_{curr} + T_{act}$ as $f_{(T_{curr}+T_{act})} = f_t + df/dt \cdot T_{act}$. If the current frequency gradient and the calculated frequency deviation ($f_{(T_{curr}+T_{act})}$) are within the active zone, the method activates the power accordingly. This way, an under- or overshooting frequency event around 50 Hz can be dampened faster, resulting in better frequency stability.

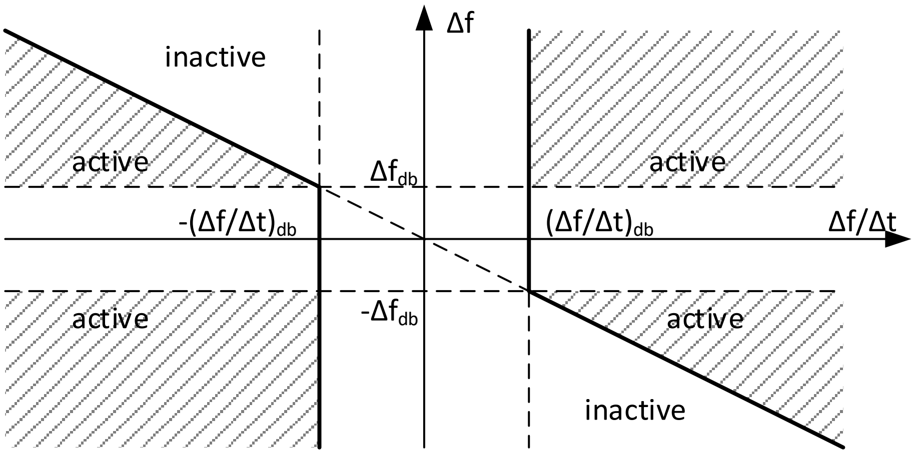

Figure 12: Improved zone-selective control of synthetic inertia (v2)

In order to illustrate the effect of this second control scheme (depicted in Figure 12), an artificial frequency event is created. This event starts with a power imbalance of 3 GW at t = 0 s, which is reduced to 1 GW at t = 30 s. The corresponding frequency and power curves are depicted in Figure 13. It is clearly visible that the improved zone-selective control activates the power faster, at both the over- and undershooting events and therefore improves frequency stability. However, in this investigated case, both control methods performed worse than the first method without zone-selective control.

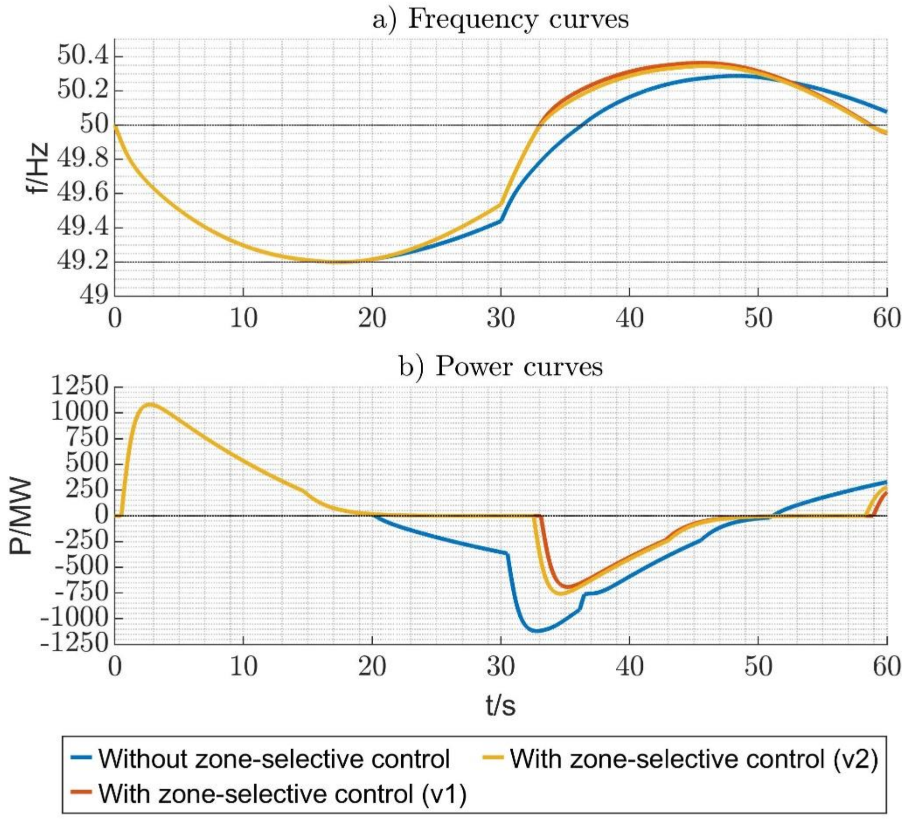

Figure 13: Frequency curves with and without zone-selective control (v1 and v2)

By introducing additional conditions for activating and deactivating the synthetic inertia power, like a certain threshold for the frequency gradient, as shown in Figure 14 with $(\Delta f/\Delta t)_{th}$, the behavior of synthetic inertia can be further improved. The corresponding frequency and power curves, with the reference values according to Table 1 and $(\Delta f/\Delta t)_{th} = 0.05\ Hz/s$, are presented in Figure 15.

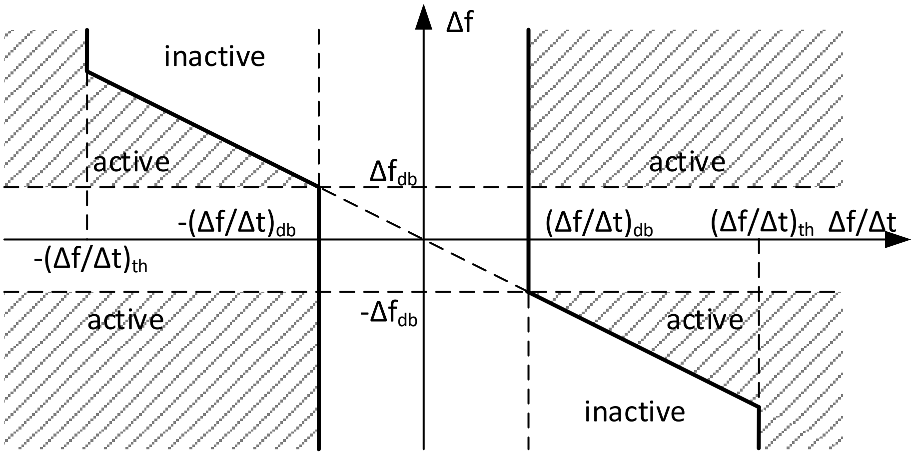

Figure 14: Improved zone-selective control of synthetic inertia with threshold (v3)

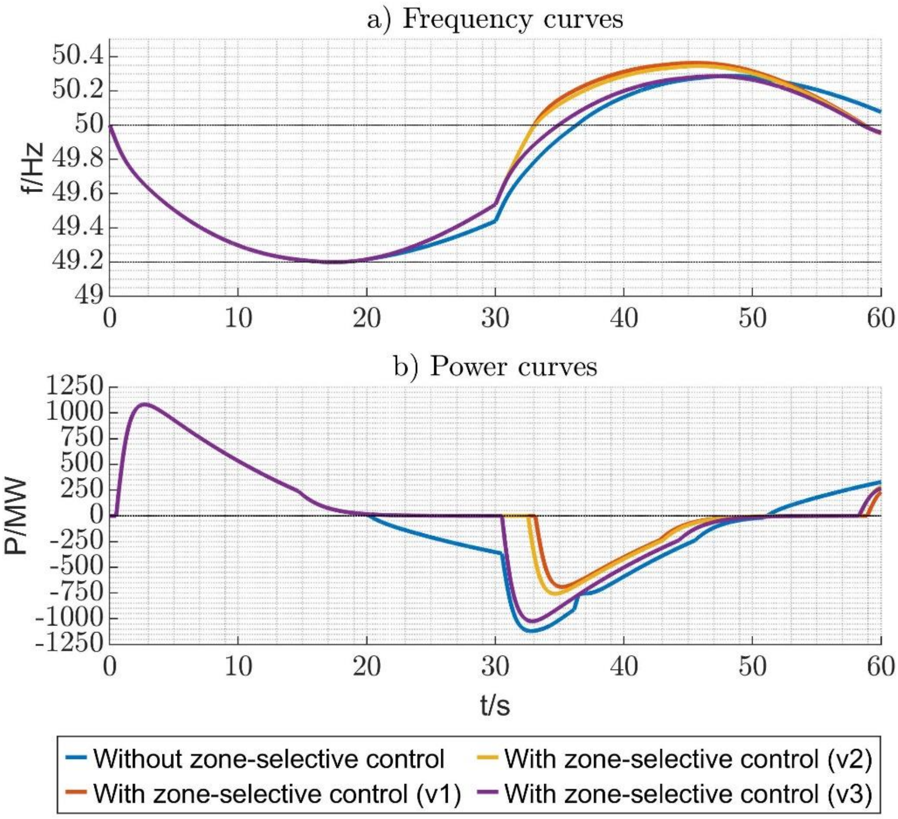

Figure 15: Frequency curves with and without zone-selective control (v1,v2 and v3)

Figure 14 shows that with the use of the third option (v3) it is possible to achieve better results than with all other options. Nevertheless, it has to be noted that the parameter $(\Delta f/\Delta t)_{th}$ was chosen deliberately to fit the selected incident. Based on the results of the sensitivity analysis regarding $(\Delta f/\Delta t)_{db}$ and especially $(\Delta f/\Delta t)_{max}$, it has to be assumed that selecting a universal value for $(\Delta f/\Delta t)_{th}$ is just as difficult, and the behavior of synthetic inertia will depend to some extent on the investigated power imbalance.

Conclusion

The increasing penetration of PEIPS raises several challenges for the operation of power systems. Together with the simultaneous decrease of the number of conventional synchronous machines, which inherently provide real inertia, this leads to a decreasing network time constant and thus a declining stability of the power system. A possible way to counteract this trend could be the rollout of synthetic inertia, provided by PEIPS. The sensitivity analysis done in this paper shows that the definition of the synthetic inertia model characteristics and the specification of its parameters, especially those regarding the frequency gradient, are not trivial tasks and require thorough research. As a possible approach to implement synthetic inertia as an improved version of real inertia provided by synchronous machines, this paper presents several options for a zone-selective control scheme. The third option of such a zone-selective control scheme with a threshold proved to be more effective, for the investigated incidents, than the first option (without zone-selective control), which aims at emulating the behavior of real inertia. However, a universal parametrization of synthetic inertia, fit for every purpose of application needs to be the topic of ongoing and future research.

Acknowledgment: This research is carried out in the frame of the research project ABS4TSO (Advanced Balancing Services for Transmission System Operators). This project is funded by the Austrian Climate and Energy Fund within the program "Energieforschung 2017". Within the scope of the ABS4TSO project, the characteristics of highly dynamic system services supporting future system stability and security in the European transmission grid will be analyzed. Especially applications like frequency stabilization via synthetic inertia, enhanced frequency response and attenuation of system oscillations are in focus. A concept for the applicability of such services and system impacts will be evaluated in field tests with a battery storage system of approx. 1MW/ 500kWh.

BIBLIOGRAPHY

[1] ENTSO-E, "High Penetration of Power Electronic Interfaced Power Sources (HPoPEIPS)," in *ENTSO-E Guidance document for national implementation for network codes on grid connection*, ed, 2017.

[2] S. Khan, B. Bletterie, A. Anta, and W. Gawlik, "On Small Signal Frequency Stability under Virtual Inertia and the Role of PLLs," *Energies 2018,* vol. 11, 2018.

[3] ENTSO-E, "European Power System 2040, Completing the map; System Needs Analysis, part of ENTSO-E's 2025, 2030, 2040 Network Development Plan 2018," 2019. [Online]. Available: https://docstore.entsoe.eu/Documents/TYNDP%20documents/TYNDP2018/european_power_system_2040.pdf.

[4] ENTSO-E, "Continental Europe Operation Handbook Appendix A1 Load-Frequency Control and Performance," 2004. [Online]. Available: https://www.entsoe.eu/fileadmin/user_upload/_library/publications/entsoe/Operation_Handbook/Policy_1_Appendix%20_final.pdf.

[5] M. Leonhardt and W. Gawlik, "Advanced Balancing Services für Übertragungsnetzbetreiber," *e&i Elektrotechnik und Informationstechnik,* vol. 136, no. 8, pp. 390-391, 2019.